

Stable isotopes of water vapor in the vadose zone: A review of measurement and modeling techniques

Keir Soderberg¹, Stephen P. Good¹, Lixin Wang² and Kelly Caylor¹

1 – Department of Civil and Environmental Engineering, Princeton University

2 – School of Civil and Environmental Engineering, University of New South Wales

Abstract

The stable isotopes of soil water vapor are useful tracers of hydrologic processes occurring in the vadose zone. The measurement of soil water vapor isotopic composition ($\delta^{18}\text{O}$, $\delta^2\text{H}$) is challenging due to difficulties inherent in sampling vadose zone airspace *in situ*. Historically, these parameters have therefore been modeled as opposed to directly measured, and typically soil water vapor is treated as being in isotopic equilibrium with liquid soil water. We present a review of the measurement and modeling of soil water vapor isotopes, with implications for studies of the soil-plant-atmosphere continuum. We also present a case study with *in situ* measurements from a soil profile in a semi-arid African savanna, which supports the assumption of liquid-vapor isotopic equilibrium. A contribution of this work is to introduce the effect of soil water potential (ψ) on kinetic fractionation during soil evaporation within the Craig-Gordon modeling framework. Including ψ in these calculations becomes important for relatively dry soils ($\psi < -10$ MPa). Additionally, we assert that the recent development of laser-based isotope analytical systems may allow for the regular *in situ* measurement of the vadose zone isotopic composition of water in the vapor phase. Wet soils pose particular sampling difficulties, and we discuss novel techniques being developed to address these issues.

24 Definitions

25 The isotope nomenclature used here is consistent with the most recent guidelines (Coplen, 2011)
26 where the decimal values are used in all calculations and “per mil” (‰) values are for display
27 purposes only. We use the term “vapor” to refer to water vapor only, and other gaseous
28 constituents are referred to as “gas”. We are explicit about the direction of the isotopic
29 fractionation factors (e.g. $\alpha_{L/V} = R_L/R_V = \varepsilon_{L/V} + 1$), and where no isotope is specified, α can refer
30 to either oxygen or hydrogen fractionation.

31

32	a_w	thermodynamic activity of water [-]
33	D	diffusion coefficient [$\text{m}^2 \text{s}^{-1}$], with subscript i indicating the minor isotopologue
34	$\delta_A, \delta_E, \delta_L, \delta_V$	relative difference of isotope ratios (e.g. $\delta^{18}\text{O} = ({}^{18}R/{}^{16}R_{\text{SMOW}} - 1)$) of the 35 atmosphere, evaporate, soil liquid, and soil vapor, respectively [-]
36	α_e, α_k	equilibrium and kinetic isotopic fractionation factor (e.g. $\alpha_{e,L/V} = R_L/R_V$) [-]
37	ε_k	kinetic isotopic fractionation ($\varepsilon_k = \alpha_k - 1$) [-]
38	e_{s0}, e_{sA}	saturation vapor pressure at the evaporating surface and in the atmosphere, 39 respectively [kPa]
40	$\theta_0, \theta_s, \theta_r$	volumetric water content of the evaporating surface, saturated and residual water 41 contents, respectively [$\text{m}^3 \text{m}^{-3}$]
42	ρ_w	density of water [kg m^{-3}]
43	‰	per mil [-]
44	ψ_0	water potential at the evaporating surface [MPa]
45	n	aerodynamic parameter for adjusting diffusivity ratios [-]

46	h_A, h_0	humidity of the atmosphere and evaporating surface; h_A' is normalized to the
47		evaporating surface [-]
48	iR_p	isotope ratio of minor isotopologue i to the abundant isotopologue in phase p
49	R	ideal gas constant [L kPa mol ⁻¹ K ⁻¹], distinguished from the isotope ratio (e.g.
50	$^{18}R_L$)	by having no superscripts or subscripts
51	T_A, T_0	temperature of the atmosphere and evaporating surface [K]

1. Introduction

Soil water dynamics are the part of the hydrologic cycle that is most directly relevant to vegetation dynamics and productivity (e.g., Rodriguez-Iturbe and Porporato, 2004). Measuring the presence, character and fate of soil water has become standard in agricultural and ecosystem science. The stable isotopes of liquid soil water are routinely measured to investigate processes related to plant water uptake such as relative rooting depth (Jackson et al., 1999), recharge rates (Cane and Clark, 1999), and hydraulic redistribution (Dawson, 1993). The isotope values of liquid soil water change in response to fractionation processes such as evaporation and condensation (Gat, 1996), and are thus dynamically linked to the isotope values of the soil water vapor. The isotopic composition of the vapor component of soil water has been much less studied than the liquid water component, mainly due to sampling difficulties. However, the recent development of laser-based isotope analysis may allow for rapid, *in situ* measurement of soil vapor isotopes. Here we review the measurement and modeling of soil water vapor isotopes, with a focus on the implications of isotope fractionation processes on our understanding of ecohydrology.

The stable isotopic composition of water (δ) is defined as $\delta = ({}^iR/{}^iR_{std} - 1)$, where iR is the ratio of a rare (denoted i , e.g., ${}^{18}\text{O}$) to common isotope (${}^2\text{H}/{}^1\text{H}$ or ${}^{18}\text{O}/{}^{16}\text{O}$) in sample water, and ${}^iR_{std}$ is the same ratio of the international standard, *VSMOW* (De Laeter et al., 2003; Gonfiantini, 1978). The stable isotope composition of water is a powerful process tracer in ecology, plant physiology, meteorology and hydrology (e.g., Brunel et al., 1992; Dawson et al., 2002; Gat, 1996; Wang et al., 2010). One of the three landmark papers that were identified in physical meteorology (Lee and Massman, 2011) is about stable isotopes of water. In this paper, Craig (1961) reported the discovery of a robust relationship between oxygen and hydrogen isotopic

abundance in precipitation, a relationship now widely known as the Global Meteoric Water Line (GMWL), which has become part of general scientific language today.

The stable isotopic composition of soil water has been used to trace water movement in the unsaturated zone (Barnes and Allison, 1988), estimate evaporation rate (Allison and Barnes, 1983) and trace groundwater recharge (Cane and Clark, 1999). The isotopic composition of water in stems and roots usually reflects the isotopic composition of plant-available soil water (Flanagan and Ehleringer, 1991; White et al., 1985), although exceptions can exist in extreme environments (Ellsworth and Williams, 2007). Thus, the isotopic composition of plant stem water has been widely used to identify plant water sources (e.g., irrigation, rainwater, groundwater) in various ecosystems (Dawson, 1996; Ehleringer and Dawson, 1992; Ehleringer et al., 1999). At the watershed scale, water isotopes can be used to trace the catchment water movement and storage mechanisms (Brooks et al., 2010). At the global scale, water isotopes can be used to explore global scale land-atmosphere interaction (Hoffmann et al., 2000), to reconstruct the past environmental parameters such as ambient temperature and relative humidity (e.g., Helliker and Richter, 2008) and to constrain primary productivity (Welp et al., 2011).

Evaporation from soil, and thus the underlying soil water vapor, can play an important role in the hydrologic cycle, particularly in dryland ecosystems (D'Odorico et al., 2007; Nicholson, 2000; Risi et al., 2010a; Yoshimura et al., 2006). These ecosystems, such as semi-arid African savannas, often have significant unvegetated patches and large diurnal and seasonal shifts in temperature and water availability leading to important feedbacks in vegetation structure (D'Odorico et al., 2007; Nicholson, 2000; Scanlon et al., 2007). For soils in wetter environments, water movement in the liquid phase is more prominent than in the vapor phase, although vapor flux out of the soil could still be a significant component of the water cycle in these

environments. These wet soils pose particular vapor sampling difficulties, which are discussed in Section 2.2.

The redistribution of soil water from wetter layers to drier layers at night (“hydraulic redistribution”) is a widespread phenomenon affecting plant community dynamics and the evaporative flux of soil water (e.g., Feddes et al., 2001; Mooney et al., 1980). However, in dry soils, diurnal shifts in soil temperature gradients can induce the movement of soil water vapor, which flows from warmer to cooler layers where it may condense (Abramova, 1969; Bittelli et al., 2008; Harmathy, 1969; Philip and de Vries, 1957) and become available to plants (Abramova, 1969). This vapor movement can occur in bare soil and have the same effect as hydraulic redistribution. For example, observations of soil water content demonstrated that the movement of water vapor in soils may enhance the ability of *Larrea tridentata* to maintain photosynthesis level at lower soil water potential (Syvertsen et al., 1975) and contribute up to 40% of hourly increases in nocturnal soil moisture within the 15–35 cm layer in a seasonally dry ponderosa pine forest (Warren et al., 2011). Soil water vapor can also be transported within the soils in response to large gradients in the salt content of the soil (Kelly and Selker, 2001). In extremely dry soils, the intrusion of atmospheric vapor into the upper few centimeters of soil and its condensation can lead to biologically significant increases in liquid soil water content (Henschel and Seely, 2008).

Land-atmosphere exchange modeling has shown that including a more spatially complex and variable evapotranspiration signal relative to precipitation improves the comparison with observations (Jouzel and Koster, 1996; Yoshimura et al., 2006). Soil water vapor isotopes can help with this parameterization through a combination of measurements and modeling. Due to practical difficulties in sampling, soil evaporation isotopic composition has traditionally been

modeled rather than measured. The most commonly used model is the Craig-Gordon model (Craig and Gordon, 1965; Horita et al., 2008) formulated to estimate equilibrium and kinetic isotopic fractionation during evaporation from the ocean surface. This model has been modified for various applications (Horita et al., 2008), and recently numerical models of isotope flux from the soil have also been developed as alternatives to Craig-Gordon (Braud et al., 2005a; Braud et al., 2009b; Haverd and Cuntz, 2010; Mathieu and Bariac, 1996; Melayah et al., 1996a). Comparisons among measured and modeled values of soil evaporate isotopic composition have shown significant deviations from Craig-Gordon (Braud et al., 2009a; Haverd et al., 2011; Rothfuss et al., 2010). Below we describe measurement and modeling techniques, and propose a modification for Craig-Gordon specific to dry soils.

2. Measurement

Measurements of soil water vapor isotopic composition are scarce (Braud et al., 2009b; Haverd et al., 2011; Mathieu and Bariac, 1996; Rothfuss et al., 2010; Stewart, 1972; Striegl, 1988) due to sampling difficulties. In this section we discuss (1) general techniques for measuring water vapor isotopic composition (cryogenic sampling and direct measurement), (2) sampling and measuring vapor in the vadose zone, (3) estimating the isotopic composition of soil evaporation flux leaving the soil surface. Table 1 lists the measurement and modeling (Section 3) methods and relevant references.

2.1 Water vapor sampling and isotope analysis

The traditional “cold trap” sampling technique for isotope analysis of water vapor involves drawing air through a tube immersed in a dry ice-alcohol mixture (for H₂O) or liquid

nitrogen (for H₂O and CO₂) where the water freezes (Dansgaard, 1953; Pollack et al., 1980; Yakir and Wang, 1996). The method has been optimized for efficiency, bringing sampling times below 15 minutes depending on the humidity level (Helliker et al., 2002), and for portability (Peters and Yakir, 2010). Another recent approach has been to use a molecular sieve to trap water vapor quantitatively, from which the collected sample is distilled in the laboratory (Han et al., 2006). The water sample then undergoes preparation and analysis – most commonly via mass spectrometry after equilibration with CO₂ for $\delta^{18}\text{O}$ determination and reduction via Zn or U for $\delta^2\text{H}$ determination, although there are many alternative preparation and sample introduction techniques, as well as new optical analytical methods available (de Groot, 2009).

Cryogenic sampling of atmospheric water vapor has been performed at various scales since the first vertical profile collections in the 1960's over North America and Europe, which included sampling in both troposphere and stratosphere (Araguas-Araguas et al., 2000; Pollack et al., 1980; Rozanski, 2005). Near-surface cryogenic atmospheric water vapor sample collections have been performed in Europe, Asia, Brazil, and Israel (Risi et al., 2010b; Rozanski, 2005; Twining et al., 2006; Yamanaka and Shimizu, 2007; Yu et al., 2005), with one group making routine collections since the early 1980s at a surface collection station in Heidelberg, Germany (Jacob and Sonntag, 1991; Rozanski, 2005).

With the development of relatively portable laser isotope analyzers (Kerstel et al., 1999), many airborne and ground-based measurements of $\delta^{18}\text{O}$ and $\delta^2\text{H}$ have been made (Griffis et al., 2010; Hanisco et al., 2007; Lee et al., 2005; Webster and Heymsfield, 2003). The laser isotope instrumentation allows for direct, rapid (1 to 10 Hz) determination of water vapor isotopic composition with uncertainties approaching those of traditional mass spectrometric methods (de Groot, 2009; Wang et al., 2009). There are now also remote sensing technologies that produce

water isotope data for the atmosphere (Worden et al., 2007), and ground-based Fourier Transform Infrared Spectroscopy (FTIR) is developing into a source of this information for the lower troposphere (Schneider et al., 2010).

2.2 Soil water vapor sampling and isotope analysis

Sampling of soil water vapor has been performed in the past using soil gas sampling apparatus and, as with atmospheric water vapor, cryogenic traps either in the laboratory (Stewart, 1972) or the field (Mathieu and Bariac, 1996; Striegl, 1988). The pioneering work of Zimmerman et al. (1967) on evaporative enrichment in liquid soil water isotopes includes an apparatus that directly collects the vapor resulting from soil evaporation, but this condensed vapor was not analyzed. Soil gas sampling via pumping is routinely performed during the monitoring and remediation of organic solvent contamination of the subsurface. The solvent sampling and pumping devices, however, are not designed for the high concentrations and low vapor pressures that characterize soil water vapor relative to organic solvents (e.g., trichloroethylene). However, the vadose zone modeling efforts surrounding soil gas sampling can help in estimating the area of influence for a given pumping rate and time span. For example, the USGS modeling framework MODFLOW now has a module for vadose zone gaseous transport (Panday and Huyakorn, 2008).

The main concern in sampling of soil water vapor for isotope analysis is the fractionation of the original isotopic composition through (1) inducing evaporation of the liquid soil water during sampling, and (2) condensing vapor inside the sampling apparatus due to the typically saturated conditions of soil water vapor (Campbell and Norman, 1998). An approach to reduce the risk of inducing evaporation is to pump at low flow rates (<200 mL/min), which has

produced reasonable results during initial testing (Section 4). Condensation in the sampling apparatus is reduced by minimizing tubing length, using all Teflon or high density polyethylene materials on wettable surfaces, and insulating or even heating the tubing if necessary (Griffis et al., 2010). In wet soils, various membranes could be used to exclude liquid water from the sampling apparatus up to a certain level of pore space saturation. Once the soils reach a low air-filled porosity level, however, authentic vapor sampling becomes impossible. At this critical level, which still needs to be determined empirically for each sampling method and soil type, liquid-vapor equilibrium needs to be assumed and the liquid itself analyzed. In a novel approach aimed at estimating this liquid soil water isotopic composition *in situ*, a membrane contactor (Membrana) has been shown to provide reliable results across a fairly wide soil temperature range (8-21°C) through the controlled evaporation of liquid soil water (Herbstritt et al., 2012).

There are two methods for estimating liquid soil water isotopic composition that are related to soil water vapor sampling. They involve sampling and analyzing CO₂ or water vapor that is in isotopic equilibrium with liquid soil water. The CO₂ sampling method is based on isotope equilibrium between soil CO₂ and liquid soil water (Scrimgeour, 1995), which has been shown to be complete below the depth of atmospheric CO₂ invasion into the soil surface (Wingate et al., 2009). This depth of invasion was found to be shallower than 5 cm in Mediterranean soils (Wingate et al., 2009), which is consistent with other investigations that found good agreement between liquid soil water and CO₂ at their shallowest depths – 20 cm (Tang and Feng, 2001) and 30 cm (Hesterberg and Siegenthaler, 1991). Interestingly, although the uncatalyzed equilibrium reaction between CO₂ and H₂O reaches equilibrium in about 3 hours (Dansgaard, 1953), the enzyme carbonic anhydrase acts as a catalyst in both plant leaves and in soil, such that $\delta^{18}\text{O}$ of CO₂ is a good tracer of photosynthetic and respiratory CO₂ exchange with

the atmosphere (Wingate et al., 2009). It is not clear whether soil water vapor plays a significant role in this reaction, but a calculation by Hsieh et al. (1998) estimates the added uncertainty due to reactions between different phases of water in the soil at 0.36 ‰ for $\delta^{18}\text{O}$. The sampling method for CO_2 is either with a chamber placed above the soil surface (e.g., Wingate et al., 2008), or a tube buried in the ground (Tang and Feng, 2001).

The second equilibration method involves placing a soil sample in a sealed plastic bag, filling the bag with dry air, and allowing the atmosphere inside the bag to reach 100% relative humidity at a constant temperature (Wassenaar et al., 2008). The bag is then punctured with a syringe connected directly to a laser isotope analyzer, the vapor is analyzed directly and its isotopic composition is used along with the equilibration temperature to calculate the soil liquid isotopic composition. This method is instructive with respect to the rate of equilibration between liquid and vapor phases – from 10 min (free water) to 3 days (clay) at 22 °C – as well as the time for the laser isotope analyzer to provide a stable signal (~300 s with a flow rate of ~150 mL/min, and a headspace of ~900 mL). For comparison with equilibration in the field, a study in volcanic soils of Hawaii estimated an *in situ* equilibration time of 48 hrs between $\delta^{18}\text{O}$ of liquid soil water and soil CO_2 (Hsieh et al., 1998). Another interesting aspect of the plastic bag equilibration method is that below 5% volumetric water content, the data was apparently not useable even though the headspace reached 100% relative humidity. This method is similar to direct equilibration of soils and plants with CO_2 and H_2 in the laboratory (Scrimgeour, 1995), which was proposed as a good method for obtaining results for very dry samples (<0.5 mL of water).

A comparison among CO_2 equilibration, vacuum distillation and azeotropic distillation found fair agreement among the methods, but also showed distinctly poor results for the CO_2 method in samples drier than about 5% moisture content (Hsieh et al., 1998). The equilibration

methods for liquid soil water are potentially quite useful in studies of plant xylem and transpired water isotopic composition in that they could provide a better representation of plant-available water than vacuum and chemical distillation methods, which are performed at elevated temperatures and thus can access more tightly bound water in the soil (Araguas-Araguas et al., 1995; Hsieh et al., 1998; Walker et al., 1994). However, further studies are needed to relate soil water held at various water potentials to plant water uptake (e.g., Brooks et al., 2010), liquid-vapor equilibration times, and liquid-vapor fractionation factors.

2.3 Measuring the isotopic composition of soil evaporation

The isotopic composition of soil evaporation can be estimated through sampling water vapor above the soil. Measurements of the near-surface atmosphere have been used for this purpose to measure vapor efflux from terrestrial ecosystems, including the “Keeling Plot” approach using gradients in isotopic composition and bulk concentration of CO₂ (Keeling, 1958), which has also been applied to water vapor (Wang et al., 2010; Yakir and Sternberg, 2000; Yepez et al., 2003). Additional methods include the Flux Gradient (Griffis et al., 2004; Yakir and Wang, 1996) and Eddy Covariance techniques (Griffis et al., 2010; Lee et al., 2005). Each of these methods involves making measurements at some altitude above the ground surface, and thus their results are applicable to a certain horizontal “footprint” from which the vapor originated. If this footprint is unvegetated, then the water vapor flux signal can be completely attributed to soil evaporation. If there is some vegetation present, however, the measured flux is from the combined evapotranspiration. Decomposing this combined signal is possible (Haverd et al., 2011; Rothfuss et al., 2010; Wang et al., 2010), but the assumptions involved in estimating the transpiration and evaporation end-members currently lead to a high degree of uncertainty.

Specifically, the isotopic end-member for transpiration represents an integrated signal weighted by the amount of transpired water delivered by each root of each transpiring plant with the active flux footprint. If the mean rooting depth changes (e.g., grasses become active), the transpiration end-member will change. Thus, characterizing this end-member through time requires regular measurement of soil water isotopic composition profiles in a way that captures heterogeneity across the footprint, as well as measurement of transpiring leaf area for plant groups with differing rooting depths (e.g., grasses, shrubs, trees). Numerical models of soil evaporation isotopic composition, discussed below, coupled with land surface dynamic models have made some advances in this field (Braud et al., 2009a; Haverd et al., 2011).

Another method for measuring soil efflux involves placing a sealed chamber over the soil, and measuring the vapors that move up into the chamber (Haverd et al., 2011; Wingate et al., 2008). The issues with this type of measurement include making a good seal with the soil surface to avoid drawing in atmospheric air, and altering the ambient conditions of the soil. If these sources of error can be minimized, chamber methods have the potential to provide good point estimates of CO₂ and H₂O releases from the soil. Chamber measurements are still challenging, however, as they necessarily change the ambient conditions, especially with respect to wind velocities and concentration gradients for the gases of interest. Improvements are still being made, particularly with open-chamber methods (Midwood et al., 2008) and open-path isotopic composition sensors (Humphries et al., 2010).

However, point estimates either with chamber methods, sampling, or *in situ* measurements, must be viewed with caution given the typically large degree of heterogeneity in a soil landscape (Ogée et al., 2004). For this reason, integrated landscape-scale estimates of soil evaporation will be more useful for investigating overall ecosystem functioning. Thus increasing

the size of an atmospheric measurement's footprint can increase its relevance for scaling up to regional and global levels. The next step towards understanding the distribution of soil evaporation isotopic composition across a wider range of temporal and spatial scales is modeling based on more readily available data (Braud et al., 2009a; Haverd et al., 2011) and improved mechanistic understanding (e.g., the effect of water potential on soil evaporation isotopic composition as proposed in this paper, Equation 9).

3. Modeling soil water vapor isotopic composition

Modeling efforts relating to soil water vapor isotopic composition (δ_V) have focused on estimating the isotopic composition of soil evaporation (δ_E), with reference to the fractionation that occurs during the evaporation of liquid soil water (δ_L). The δ_E modeling has typically been performed in the framework of open-water evaporative fractionation developed by Craig and Gordon (1965), and recently numerical isotope transport models have been developed as an alternative (Braud et al., 2009a; Braud et al., 2005a; Haverd and Cuntz, 2010; Mathieu and Bariac, 1996; Melayah et al., 1996a; Shurbaji and Phillips, 1995). Here we present a discussion of (1) equilibrium isotope fractionation between liquid and vapor forms of water from theoretical and empirical perspectives, (2) evaporative fractionation and the Craig-Gordon (CG) model, and (3) soil water vapor isotope models including modified CG and isotope transport models.

3.1 Liquid-vapor equilibrium isotopic fractionation

Every isotope fractionation model relies on estimates of the liquid-vapor equilibrium fractionation factors ($\alpha_{e,L/V}(^{18}O)$ and $\alpha_{e,L/V}(^2H)$; Equation 1), and how this parameter changes under different environmental conditions. Temperature is the environmental parameter used for

the $\alpha_{e,L/V}$ estimates, and this relationship ($\alpha_{e,L/V}-T$) has been well characterized experimentally (Horita and Wesolowski, 1994; Majoube, 1971). Efforts to model the underlying processes of the $\alpha_{e,L/V}-T$ relationship from theory (Chialvo and Horita, 2009; Oi, 2003) have not improved on the empirical relationships that have been implemented in studies of evaporation for more than four decades (Horita et al., 2008). Thermodynamic modeling based on Equations of State for various water molecule isotopologues, captures the purely empirical relationships well (Japas et al., 1995; Polyakov et al., 2007). The $\alpha_{e,L/V}-T$ relationship has only been modified slightly since (Majoube, 1971) to cover a larger temperature range (Horita and Wesolowski, 1994), with the current formulations given in Equations 2 and 3.

$$\alpha_{e,L/V}(^{18}O) = \frac{{}^{18}R_L}{{}^{18}R_V} \quad [\text{Equation 1}]$$

$$10^3 \ln \alpha_{e,L/V}(^{18}O) = -7.685 + 6.7123 \left(\frac{10^3}{T} \right) - 1.6664 \left(\frac{10^6}{T^2} \right) + 0.35041 \left(\frac{10^9}{T^3} \right) \quad [\text{Equation 2}]$$

$$10^3 \ln \alpha_{e,L/V}(^2H) = 1158.8 \left(\frac{T^3}{10^9} \right) - 1620.1 \left(\frac{T^2}{10^6} \right) + 794.84 \left(\frac{T}{10^3} \right) - 161.04 + 2.9992 \left(\frac{10^9}{T^3} \right)$$

[Equation 3]

Three modeling approaches using (1) molecular simulation, (2) theoretical (“*ab initio*”) calculations and (3) thermodynamics have recently been compiled to examine the effects of isotopic substitutions on the properties of the water molecule (Chialvo and Horita, 2009). These three approaches capture the shape of the observed $\alpha_{e,L/V}-T$ relationships (Equations 2 and 3), but the difference among the models is large relative to the level of fractionation seen empirically (Table 2). Molecular modeling is used by chemists as a supplement to experimentation in an

effort to understand the underlying dynamics in chemical reactions. Various modeling approaches are used to depict electron densities and molecular orbital dynamics based on energies associated with all bonded and non-bonded atomic interactions.

Using molecular-based simulation, $\alpha_{e,L/V}$ was estimated based on two contrasting models of the water molecule: Gaussian charge polarizable (GCP) and nonpolarizable extended simple point charge (SPC/E). The GCP model performed better than SPC/E, but produced fractionation factors ($\alpha_{e,L/V}$) around 5 ‰ higher for $\alpha_{e,L/V}(^{18}O)$ and 500 ‰ higher for $\alpha_{e,L/V}(^2H)$ than those $\alpha_{e,L/V}$ values found experimentally at 25 °C (Horita and Wesolowski, 1994; Majoube, 1971). Chialvo and Horita (2009) recognized the large deviations of their models from experimental data, and suggested a parameterization of their $\alpha_{e,L/V}$ - T relationship that will allow for experimental data to create more accurate molecular dynamics models in the future. Two *ab initio* (“from first principles”) models using molecular orbital calculations performed somewhat better relative to empirical data, within 4 ‰ for $\alpha_{e,L/V}(^{18}O)$ and 66 ‰ for $\alpha_{e,L/V}(^2H)$ (Oi, 2003).

Lastly, two thermodynamic modeling efforts produced much better results applying solute dissolution (Japas et al., 1995) and corresponding states principle (Polyakov et al., 2007) approaches, apparently with deviations from empirical data of less than 0.1 ‰ and 1 ‰ for $\alpha_{e,L/V}(^{18}O)$ and $\alpha_{e,L/V}(^2H)$, respectively, at typical environmental temperatures. Despite their different approaches, these two thermodynamic models show very good agreement with each other, especially below 50 °C. These approaches do incorporate some empirical data – e.g., vapor pressures for solutions of pure isotopically substituted water (D₂O and H₂¹⁸O).

Overall, the somewhat empirical thermodynamic modeling (Japas et al., 1995; Polyakov et al., 2007) performed much better than the purely theoretical *ab initio* (Oi, 2003) and molecular simulation (Chialvo and Horita, 2009) models. Most importantly, all three approaches, in spite of

drastic differences in $\alpha_{e,L/V}$, show the same shape and limit characteristics. Therefore these models have the potential to provide insight into the underlying mechanisms of the robust empirical $\alpha_{e,L/V}$ - T relationships (Equations 2 and 3), which are still preferred for estimating $\alpha_{e,L/V}$ (Gat, 1996; Horita et al., 2008; Kim and Lee, 2011).

3.2 Isotopic fractionation during evaporation from free water

The empirical $\alpha_{e,L/V}$ values discussed above can be used to calculate the isotopic composition of vapor that is in isotopic equilibrium with liquid water at a given temperature. This equilibrium is most likely reached in soil pore spaces where sufficient moisture is available (Braud et al., 2005a; Braud et al., 2005b; Mathieu and Bariac, 1996), as is illustrated with a case study in Section 4. The fractionation during evaporation from a free surface (e.g., the ocean), involves both equilibrium (α_e) and kinetic (α_k) fractionation, and will be described here as a basis for the soil evaporation discussion that follows.

Modeling efforts that include both equilibrium and kinetic fractionation were motivated by early observations of marine water vapor being isotopically depleted relative to the equilibrium fractionation factor for a given temperature (Craig and Gordon, 1965). Thus, in addition to $\alpha_{e,L/V}$ for a given temperature at the evaporating surface (T_0), the parameters required for the estimation of the kinetic fractionation include relative humidity (h), diffusivity ratios of the isotopologues of interest (D/D_i), and an aerodynamic parameter (n , Table 3). The variability in these kinetic parameters is dominated by relative humidity of the air into which the water is evaporating (h_A), which must be recalculated (h_A') from the measured value at some height above the evaporating surface based on the temperature and activity of water at the evaporating surface (Craig and Gordon, 1965; Horita, 2005; Horita et al., 2008; Sofer and Gat, 1975). The overall

relationship (Equations 4, 5 and 6) was first described by Craig and Gordon (1965) and is still used to estimate isotopic fractionation during evaporation from both a free surface and soil (Gat, 1996; Horita et al., 2008), with modifications specific to soil evaporation described in the next section. As summarized in Horita et al. (2008), the CG model is a physically-based model where the air-water interface is at isotopic equilibrium. Above this interface is a laminar flow layer of variable thickness, which accounts for additional fractionation due to differences in molecular diffusivities of isotopologues. This laminar layer is followed by a turbulent mixing layer, which does not contribute to isotope fractionation.

$$\delta_E = \frac{\delta_L / \alpha_{e,L/V} - h'_A \delta_A - (\alpha_{e,L/V} - 1) - \varepsilon_{k,L/V}}{1 - h'_A + \varepsilon_{k,L/V}} \quad [\text{Equation 4}]$$

$$\varepsilon_{k,L/V} = n(1 - h'_A) \left(\frac{D}{D_i} - 1 \right) \frac{r_m}{r} \quad [\text{Equation 5}]$$

$$h'_A = \frac{h_A e_{sA}}{a_w e_{s0}} \quad [\text{Equation 6}]$$

The “weighting term” r_m/r is assumed to be 1 for small water bodies, but can reach 0.5 for strongly evaporating systems like the Mediterranean Sea (Gat, 1996). The effect of the aerodynamic parameter n ($n = 0.5$ for free water, 1 for completely laminar flow as in very dry soil, see below) is to reduce the kinetic fractionation due to the reduced role of molecular diffusion when the turbulent layer interacts strongly with the evaporating surface. Higher humidity leads to reduced kinetic fractionation, but its overall effect on δ_E is not straightforward because an increased h'_A leads to both a lower numerator and a lower denominator in Equation 4. Interestingly, the thermodynamic activity of water (a_w , between ~ 0.6 in brines to 1 in fresh

water) acts to increase the normalized humidity h_A' for evaporation from saline water. The same is true for evaporation from soils, as introduced below (Equation 9), when soil water potential is used to calculate the activity of soil water. Thus, a reduced activity of water leads to limited evaporative enrichment in saline water relative to fresh water exposed to the same conditions (Horita, 2005). The necessary field measurements to make a CG calculation are discussed with the case study in Section 4. The appropriate height for making the atmospheric measurements is above the turbulent mixing layer, given that these values are meant to represent “free atmosphere” (Craig and Gordon, 1965; Horita et al., 2008), although this condition is most likely not fully satisfied for many applications of the CG model.

In addition to normalized humidity, the representation of diffusive fractionation has a great effect on δ_E modeled from CG (Braud et al., 2009a). Cappa et al. (2003) provided significantly revised diffusivities of water isotopologues (D/D_i in Equation 7, Table 2) based on gas kinetic theory as well as experimental results, and emphasize the use of skin temperature rather than bulk temperature for fractionation calculations. However, evidence for surface cooling during evaporation from natural water bodies is not yet available. Thus, the diffusivities of Merlivat (1978) are still generally preferred (Lee et al., 2007). Recent evaluations and experimental results from Luz et al. (2009) have also suggested that the Merlivat (1978) values are still valid. However, if an evaporating body is not well mixed, lower temperatures apparently do develop in the top 0.5 mm, and if this temperature structure persists, Cappa et al. (2003) clearly showed that diffusivities and associated kinetic fractionation factors can be quite different from those calculated based on the temperature of the bulk water. This enhanced fractionation may be counteracted by the accumulation of enriched isotopologues at the surface, given the lack of mixing required for significant surface cooling to occur (Horita et al., 2008).

3.3 Modeling the isotopic composition of soil water vapor and soil evaporation

Due to the difficulty in soil water vapor isotope (δ_V) sampling in the past, there is little information on δ_V directly collected from soil profiles (Mathieu and Bariac, 1996). Direct measurements of *in situ* soil water vapor δ_V are now possible and will provide a direct check for the utilization of the CG model in various conditions especially for dry soils. An important missing component in the application of the CG model to soil evaporation is the effect of water potential on the activity of water, which can be easily incorporated with measurements of soil moisture or soil water potential, as developed below.

In recent years, transport-based isotope models such as SiSPAT-isotope model (Braud et al., 2009a; Braud et al., 2005a) and Soil-Litter-Iso model (Haverd and Cuntz, 2010; Haverd et al., 2011) have been developed to model soil δ_E , building from analytical solutions for idealized cases that were developed previously (Barnes and Allison, 1983). The Soil-Litter-Iso model was compared with other analytical frameworks (Haverd and Cuntz, 2010), and recent testing of the model against water vapor isotopic composition data from a chamber placed on top of the soil yielded very promising results. The model captures diurnal patterns and a 10-day dry-down quite well, although a mean deviation of around 10 ‰ was observed for $\delta^2\text{H}$ between measured and modeled values (Haverd et al., 2011). SiSPAT-isotope model was tested using laboratory column setup and parameters were calibrated to maximize the model-data agreements. The results indicate that the evaporative enrichment process is very sensitive to changes in kinetic fractionation (Braud et al., 2009a).

The numerical models have introduced many important soil parameters such as the soil moisture, tortuosity, and water potential, which are not explicitly considered in the CG modeling

framework. The effect of these parameters could be lumped into the kinetic isotope fractionation factor (α_k) to improve the agreement between model output and observational data for each time step and soil layer in the model. The missing key component to test these effects is the direct measurement of δ_E and authentic δ_{SV} measurements. The mass-balance framework developed in Wang et al. (2012) for direct and continuous quantification of the isotopic composition of leaf transpiration could be adopted for quantifying soil δ_E from measurements, which then can be verified using authentic *in situ* soil water vapor δ_V measurements.

The surface boundary condition of the most recent bare soil evaporation numerical model provides an isotope evaporative flux based on equilibrium (α_e) and kinetic fractionation (α_k) factors, as well as heat and moisture conservation equations solved for the soil-air interface (Haverd and Cuntz, 2010). The α_k calculation involves adjusting the molecular diffusivity ratio of isotopologues by the aerodynamic parameter n (Equation 7), analogous to Equation 5.

$$\alpha_{k,L/V} = \left(\frac{D_i}{D} \right)^n \quad \text{[Equation 7]}$$

This equation has taken on various forms in models, as summarized and evaluated by Braud et al. (2005b). In an attempt to incorporate the laminar flow development of the soil as it dries, n is related to volumetric soil moisture (θ) as first proposed by Mathieu and Bariac (1996) and adopted in subsequent numerical models (Braud et al., 2009a; Braud et al., 2005b; Haverd and Cuntz, 2010). This relationship (Equation 8) allows for n to vary between 0.5 for saturated conditions and 1 for dry soil (“residual” soil moisture) where the laminar layer will have fully developed.

461

$$n = \frac{(\theta_0 - \theta_r)n_a + (\theta_s - \theta_0)n_s}{\theta_s - \theta_r} \quad [\text{Equation 8}]$$

463

464 Where $n_a = 0.5$ and $n_s = 1$, and subscripts s , r , and θ refer to saturated, residual and ambient
 465 conditions at the evaporating surface, respectively. In the original formulation θ_r was defined as
 466 the minimum soil moisture reached when the soil is in equilibrium with the atmosphere (Mathieu
 467 and Bariac, 1996).

468 The numerical models also include the humidity of the soil modeled from soil water
 469 potential as part of their evaporative flux formulation (Braud et al., 2009a; Braud et al., 2005a;
 470 Mathieu and Bariac, 1996). However, they do not take into account the relationship between
 471 water potential and the activity of the water, a_w , which is provided by the Kelvin equation
 472 (Equation 9; Barnes and Gentle, 2011; Gee et al., 1992).

473

$$\ln(a_w) = \frac{\psi_0 M_w}{RT_0 \rho_w} \quad [\text{Equation 9}]$$

475

476 where ψ_0 is soil water potential [kPa] of the evaporating surface, M_w is the molecular weight of
 477 water (18.0148 [g mol⁻¹]), R is the ideal gas constant (8.3145 [mL MPa mol⁻¹ K⁻¹]), ρ_w is the
 478 density of water, and T_0 is the temperature [K] of the evaporating surface.

479 The activity of water is equivalent to the relative humidity in the soil under liquid-vapor
 480 equilibrium, a relationship that is commonly used to measure water potential in soils through
 481 devices that measure the dew point in a sealed chamber that contains a soil sample (Gee et al.,
 482 1992). When considered with the CG model framework, a reduction in a_w increases the

normalized humidity h_A' (Equation 6), reducing $\varepsilon_{k,L/V}$ (Equation 5), ultimately affecting the δ_E calculation (Equation 4). This modification of h_A' is identical to the normalization using the activity of water in saline waters (Horita et al., 2008). Thus, it can be easily incorporated into CG formulations by combining Equations 6 and 9. The effect of including the water potential in a CG model calculation of δ_E is illustrated with measurements of a soil profile at Mpala Research Center, Kenya described in Section 4 below.

In addition to the effects of water potential on fractionation during evaporation, the relationship between equilibrium fractionation in soils and water potential has yet to be rigorously described. There are strong indications from the equilibration of CO_2 with soil water that dry soils exhibit a different equilibrium behavior than wet soils (Hsieh et al., 1998; Wassenaar et al., 2008). In reviewing some field collections of soil water vapor, Mathieu and Bariac (1996) commented that in dry soils the observed vapor was more enriched than would be expected from equilibrium fractionation at the given temperature. Changes in water structure and properties such as vapor pressure due to confinement in small spaces such as soil pores have been recently reported for bulk water in carbon nanotubes (Chaplin, 2010) and for hydrogen isotopes in water adsorbed to porous silica tubes, leading to significant differences in equilibrium isotope fractionation between liquid and vapor phases (Richard et al., 2007).

An interesting early experiment on water isotopic fractionation in clays (Stewart, 1972) used a saturated KCl solution as the moisture source for vapor that was allowed to equilibrate with a thin layer of dried clay. In this KCl-vapor-clay system, a wide range of isotopic fractionation factors was observed ($\alpha_{L/V}({}^2\text{H})_{\text{clay}} = 0.93$ to 1.06 , with a median of 1.04 ; HDO concentration ratios of Stewart (1972) were divided by the estimated $\alpha_{L/V}({}^2\text{H})_{\text{KCl}} = 1.06$). The temperatures weren't controlled, and a value of $\alpha_{L/V}({}^2\text{H})_{\text{KCl}}$ as low as 1.06 would require a

temperature >40 °C using Equation 3 (Horita and Wesolowski, 1994). Nevertheless, the indication is that $\alpha_{L/V}(^2H)_{clay}$ can have a wide range, but with values below the isotopic fractionation factor for free water at a given temperature. Interestingly, the recent analogous work with porous silica tubes instead of clays (Richard et al., 2007) found $\alpha_{L/V}(^2H)$ values of around 1.03 at 20 % relative humidity and 1.05 at 80 % relative humidity at around 20 °C, compared with 1.085 from Equation 3. Thus, these results are somewhat consistent with the less-controlled early study with clays, suggesting that the equilibrium isotopic fractionation between vapor and water adsorbed on clays is lower than the free water value at the same temperature.

A final consideration towards understanding the isotopic composition of soil water vapor is the organization of water molecules within the liquid phase. It has been shown that enriched isotopologues exist at higher concentrations near dissolved ions, and thus near particle surfaces (Phillips and Bentley, 1987). Given this structure, there could potentially be a concentration of depleted isotopes near the evaporating surface of porewater. This “hydration sphere isotope effect” would cause isotopic differences between bulk water and the evaporating surface and require a stagnant solution, similar to the skin temperature effect shown by Cappa et al. (2003). The impact of isotopic gradients within individual pockets of liquid soil water on δ_E has not been explored. If an isotopic difference exists between bulk water and the evaporating surface, this could be another reason to use equilibration analytical methods on undisturbed soils for estimating liquid isotopic composition (Herbstritt et al., 2012; Hsieh et al., 1998; Scrimgeour, 1995; Wassenaar et al., 2008).

The isotopic composition of soil evaporation is the result of several different fractionation processes. First, the phase change and equilibrium processes within the soil matrix are governed by temperature and soil water potential. Kinetic fractionation is affected by physical

characteristics of the diffusion path (e.g. tortuosity) as well as isotopic gradients between the site of evaporation and the initiation of turbulent mixing just above the soil surface. Vapor moving vertically through the soil will also likely re-equilibrate with the liquid water along its path. The overall apparent fractionation between liquid water at any given depth and the resultant evaporative flux leaving the soil surface reflects all of these fractionation processes. As the liquid water sources for soil evaporation fluctuate in depth and isotopic composition, modeling the soil evaporation isotopic end-member accurately at any given time becomes very difficult. Thus, techniques for measuring the evaporated vapor itself will be very important as this field moves forward. In the next section we provide an example of one step in this direction: direct measurements within the soil matrix.

4. Case Study: Soil water vapor in an African savanna

An example of direct soil water vapor isotope measurement is shown in Figure 1, with data from a single profile collected at Mpala Research Centre, Kenya, on 29 March 2011 from 12:45 to 13:00 local time. The soil is a red sandy loam with a bulk density of $1.45 \text{ [g cm}^{-3}\text{]}$ and a porosity of 0.45. The vegetation is mixed semi-arid savanna, and the local mean annual precipitation is around 600 mm. Soil vapor was sampled at four depths (5, 10, 20 and 30 cm; sampled in depth order starting with 5 cm) via buried Teflon tubing, with the final 10 cm of each tube perforated and packed with glass wool. Soil vapor was drawn directly into a laser water vapor isotope analyzer (DLT100, Los Gatos Research Inc., Mountain View, CA) at a flow rate of 150-180 mL/min, diluted with ambient air (intake at 2 m above ground) for a total flow of 400 mL/min. This dilution allowed for reduced flow rates at the soil vapor intakes and lowered the humidity in the tubing and analytical equipment to reduce the chance of forming condensation.

Data was collected for around 90 seconds at each depth. Soil temperature was measured with TCAV averaging soil temperature probes (Campbell Scientific Inc., Logan, UT) at 5 and 20 cm, and a linear profile was assumed for 10 and 30 cm. Ambient atmospheric water vapor isotopic composition, humidity and temperature were sampled at 2 m above the ground surface. Soil samples were collected from an auger hole adjacent to the buried tubing immediately after vapor sampling. Water potential was measured via a dew point potentiometer (WP4T, Decagon Devices Inc., Pullman, WA). Liquid soil water was isolated via cryogenic vacuum distillation (West et al., 2006) and analyzed with a continuous-flow water vapor isotope analyzer using a heated nebulizer for sample introduction (WVSS, Los Gatos Research, Inc.).

Equilibrium water vapor isotopic compositions were calculated for each depth based on the respective measured liquid soil water isotopic composition, soil temperature and the associated fractionation factors (Equations 1 to 3). For each depth, the corresponding CG modeled values were calculated in two ways: (1) conventionally, using Equations 2 to 8 assuming $a_w=1$ (Figure 1 and Table 3, $\delta_E(\theta, T)$); (2) including soil water potential by calculating a_w with Equation 9 ($\delta_E(\theta, T, \psi)$). The parameters for CG calculations are given in Table 3 with specific examples and typical ranges.

The measured soil vapor isotope values fell close to those that would be expected for isotopic equilibrium at the temperature for each depth (Figure 1). The measured values cover a reduced range (-4.0 to -2.2 ‰ for $\delta^{18}\text{O}$) relative to the equilibrium values (-7.5 to 4.1 ‰ for $\delta^{18}\text{O}$), but have similar mean values of -2.8 ‰ and -3.0 ‰ for $\delta^{18}\text{O}$ and -57 ‰ and -65 ‰ for $\delta^2\text{H}$, respectively. These mean values are weighted by soil moisture contents (θ_0) of 5.3, 6.0, 6.2, and 6.6 vol% for 5, 10, 20 and 30 cm, respectively. The fact that the measured vapor isotope values fall in a smaller range, but within the calculated equilibrium values, suggests that either

the sampling process induced mixing of vapor from various depths, or that the vapor is somewhat mixed within the sampling depths at this time of day. Sampling-induced mixing is likely given that around 0.5 to 0.6 L of soil were influenced by the sampling at each depth. Subtracting volumetric water contents from a porosity of 0.45 gives air-filled porosity values of 0.38 to 0.39, resulting in a radius of influence of about 7 cm around each perforated section of tubing, suggesting that the sampling depths overlap to some degree. The three sets of values – liquid, measured vapor and equilibrium vapor – have similar slopes of 3.1, 3.4, and 3.0 ($\delta^2\text{H}$ vs. $\delta^{18}\text{O}$). Although this level of consistency among slopes is encouraging within the scope of the present study, a second study is needed to examine the differences in these slopes relative to differences in fractionation factors as well as the combined uncertainties in $\delta^2\text{H}$ and $\delta^{18}\text{O}$. Interestingly, the measured soil water vapor isotope values are much closer to the equilibrium vapor isotope values than the CG modeled δ_E values (Figure 1). This example is therefore consistent with the typical assumption of isotopic equilibrium between liquid and vapor in the soil (e.g., Mathieu and Bariac, 1996).

The effect of including water activity (i.e., soil water potential, ψ) in the CG calculations depends on the relationships among equilibrium vapor, ambient vapor, and ambient humidity. To examine these relationships as well as the effect of including soil water content (θ), we made a series of CG calculations starting with the 5 cm depth parameters of Figure 1 and Table 3. We varied ψ_0 and calculated θ_0 using a relationship of the form:

$$\theta = \left(\frac{a}{-\psi} \right)^{1/b} \quad \text{[Equation 10]}$$

where $a = 0.00109$ and $b = 3.46$, based on 410 paired measurements of ψ and θ for 14 separate drying experiments. The measured values ranged from -0.2 MPa to -61 MPa for ψ and 1 vol% to 41 vol% for θ .

We then calculated δ_E using Equations 2 to 9 (Figure 2, solid black lines). We also varied three atmospheric parameters T_A , δ_A and h_A (Figure 2, dashed black lines). Lastly, we made the same calculations without considering θ (i.e., $n = 1$) or ψ (i.e., $a_w = 1$), and used both conventional (Merlivat, 1978) and revised (Cappa et al., 2003) values for equilibrium isotope fractionation factors (Figure 2, gray lines). From these calculations it is clear that for drying soils, the effect of including ψ can be similar to or greater than the effect of including θ (i.e., changing n from 0.5 to 1). Including θ (Equation 8), which leads to $n=0.5$ in the wettest soils (θ_0 close to 0 MPa), leads to more enriched δ_E values in wetter soils. Including ψ (Equation 9) apparently leads to the opposite effect, with more enriched δ_E values in drier soils. Both mechanisms can be correct, with the former (lower n and higher δ_E in wetter soils) describing the decrease in kinetic fractionation as the soil evaporation becomes more controlled by atmospheric turbulence than by diffusion in the soil (Mathieu and Bariac, 1996). The latter (higher h_A' and higher δ_E in drier soils) simply describes the effect of lower water activity on the saturation vapor pressure in the soil. This soil water potential effect can also be as large as the impact of using the drastically different diffusivity ratios of Cappa et al. (2003) rather than those of (Merlivat, 1978).

5. Conclusions

We summarized all the available modeling and field methods to quantify isotopic composition of water vapor, with a focus on the Soil-Plant-Atmosphere Continuum. When

applying the Craig-Gordon (CG) modeling framework to soil evaporation, we suggest the inclusion of soil water potential in the normalization of “free atmosphere” humidity to the evaporating surface (Equations 6 and 9), just as water activity is included in the normalization for evaporation from saline waters. This will reduce the total fractionation for evaporation from unsaturated soils as predicted by the CG model. Such a reduction is consistent with observations of enriched soil water vapor, and can be significant in soils with water potentials drier than around -10 MPa. This improvement is easily implemented in all CG formulations, and the only additional measurement required is soil water potential. This parameter can also be calculated from soil water content using an appropriate soil water retention curve. There is also a possibility that leaf water potential could be used to improve the use of normalized humidity in application of the CG model to evaporative isotopic enrichment in leaves (e.g., Cuntz et al., 2007), although leaf water potential is highly variable and more difficult to estimate than soil water potential.

Another feature of isotopic fractionation in soil water that is likely to change through experimentation is the equilibrium fractionation factor. The equilibrium fractionation for free water is still represented empirically. The indication from experiments between vapor and water adsorbed onto clay and silica tubes is that liquid-vapor equilibrium fractionation is substantially reduced in a porous media setting relative to free water. The structure of water changes in confined spaces, and it is expected that the nature of pore spaces in different types of soils will lead to different equilibrium fractionation factors. The use of stable isotopes of water vapor in understanding the Soil-Plant-Atmosphere Continuum at various scales depends on an accurate understanding of fractionation processes and the associated modeling of isotopic fluxes in the environment. The relatively new analytical capabilities for water vapor isotopes coupled with

642 novel sampling approaches under development will provide the necessary data to follow these
643 fractionation processes *in situ*.

644

645 Acknowledgements

646 This project was funded by NSF through a CAREER award to K. K. Caylor (EAR847368). Lixin
647 Wang also acknowledges the financial support from the vice-chancellor's postdoctoral research
648 fellowship at the University of New South Wales. We greatly appreciate the field and laboratory
649 assistance of Ekomwa Akuwam, John Maina Gitonga and the staff at Mpala Research Centre.

650

References

- Abramova, M.M. 1969. Movement of moisture as liquid and vapor in soils of semi-deserts. In: P. E. Rytema and H. Wassink, editors, Wageningen Symposium on Water in the Unsaturated Zone. IASH-UNESCO, Gentbrugge - Paris. p. 781-789.
- Allison, G.B. and C.J. Barnes. 1983. Estimation of Evaporation from Non-Vegetated Surfaces Using Natural Deuterium. *Nature* 301: 143-145.
- Araguas-Araguas, L., K. Froehlich and K. Rozanski. 2000. Deuterium and oxygen-18 isotope composition of precipitation and atmospheric moisture. *Hydrological Processes* 14: 1341-1355.
- Araguas-Araguas, L., K. Rozanski, R. Gonfiantini and D. Louvat. 1995. Isotope Effects Accompanying Vacuum Extraction of Soil-Water for Stable-Isotope Analyses. *Journal of Hydrology* 168: 159-171.
- Barnes, C.J. and G.B. Allison. 1983. The distribution of deuterium and ^{18}O in dry soils 1. Theory. *Journal of Hydrology* 60: 141-156.
- Barnes, C.J. and G.B. Allison. 1988. Tracing of Water-Movement in the Unsaturated Zone Using Stable Isotopes of Hydrogen and Oxygen. *Journal of Hydrology* 100: 143-176.
- Barnes, G. and I. Gentle. 2011. *Introduction to Interfacial Science* Oxford University Press, Oxford.
- Bittelli, M., F. Ventura, G.S. Campbell, R.L. Snyder, F. Gallegati and P.R. Pisa. 2008. Coupling of heat, water vapor, and liquid water fluxes to compute evaporation in bare soils. *Journal of Hydrology* 362: 191-205.

672 Braud, I., T. Bariac, P. Biron and M. Vauclin. 2009a. Isotopic composition of bare soil
 673 evaporated water vapor. Part II: Modeling of RUBIC IV experimental results. Journal of
 674 Hydrology 369: 17-29. doi:10.1016/j.jhydrol.2009.01.038.

675 Braud, I., T. Bariac, J.-P. Gaudet and M. Vauclin. 2005a. SiSPAT-Isotope, a coupled heat, water
 676 and stable isotope (HDO and H₂¹⁸O) transport model for bare soil. Part I. Model
 677 description and first verifications. Journal of Hydrology 309: 277-300.

678 Braud, I., T. Bariac, M. Vauclin, Z. Boujamlaoui, J.-P. Gaudet, P. Biron, et al. 2005b. SiSPAT-
 679 Isotope, a coupled heat, water and stable isotope (HDO and H₂¹⁸O) transport model for
 680 bare soil. Part II. Evaluation and sensitivity tests using two laboratory data sets. Journal
 681 of Hydrology 309: 301-320.

682 Braud, I., P. Biron, T. Bariac, P. Richard, L. Canale, J.P. Gaudet, et al. 2009b. Isotopic
 683 composition of bare soil evaporated water vapor. Part I: RUBIC IV experimental setup
 684 and results. Journal of Hydrology 369: 1-16. doi:10.1016/j.jhydrol.2009.01.034.

685 Brooks, J.R.e., H.R. Barnard, R. Coulombe and J.J. McDonnell. 2010. Ecohydrologic separation
 686 of water between trees and streams in a Mediterranean climate. Nature Geoscience 3:
 687 100-104, doi:110.1038/ngeo1722.

688 Brunel, J.P., H.J. Simpson, A.L. Herczeg, R. Whitehead and G.R. Walker. 1992. Stable isotope
 689 composition of water vapor as an indicator of transpiration fluxes from rice crops. Water
 690 Resources Research 28: 1407-1416.

691 Campbell, G.S. and J.M. Norman. 1998. An introduction to environmental biophysicsSpringer,
 692 New York.

693 Cane, G. and I.D. Clark. 1999. Tracing ground water recharge in an agricultural watershed with
 694 isotopes. Ground Water 37: 133-139.

695 Cappa, C.D., M.B. Hendricks, D.J. DePaolo and R.C. Cohen. 2003. Isotopic fractionation of
696 water during evaporation. *Journal of Geophysical Research* 108: 4525.

697 Chaplin, M.F. 2010. Structuring and behavior of water in nanochannels and confined spaces. In:
698 L. J. Dunne and G. Manos, editors, *Adsorption and Phase Behavior in Nanochannels and*
699 *Nanotubes*. Springer, New York. p. 241-255.

700 Chialvo, A.A. and J. Horita. 2009. Liquid-vapor equilibrium isotopic fractionation of water: How
701 well can classical water models predict it? *The Journal of Chemical Physics* 130: 094509.

702 Coplen, T.B. 2011. Guidelines and recommended terms for expression of stable isotope-ratio and
703 gas-ratio measurement results. *Rapid Communications in Mass Spectrometry* 25: 2538-
704 2560.

705 Craig, H. 1961. Isotopic variations in meteoric waters. *Science* 133: 1702-1703.

706 E. Tongiorgi. 1965. Deuterium and oxygen-18 variations in the ocean and marine atmosphere.
707 *Stable isotopes in oceanographic studies and paleotemperatures*, Pisa. Laboratory of
708 *Geology and Nuclear Science*.

709 Cuntz, M., J. Ogée, G. Farquhar, P. Peylin and L.A. Cernusak. 2007. Modelling advection and
710 diffusion of water isotopologues in leaves. *Plant Cell and Environment* 30: 892-909.

711 D'Odorico, P., K. Caylor, G.S. Okin and T.M. Scanlon. 2007. On soil moisture-vegetation
712 feedbacks and their possible effects on the dynamics of dryland ecosystems. *Journal of*
713 *Geophysical Research* 112: G04010.

714 Dansgaard, W. 1953. The abundance of ^{18}O in atmospheric water and water vapor. *Tellus* 5: 461-
715 469.

716 Dawson, T.E. 1993. Hydraulic Lift and water-use by plants: Implications for water-balance,
717 performance and plant-plant interactions. *Oecologia* 95: 565-574.

Dawson, T.E. 1996. Determining water use by trees and forests from isotopic, energy balance
 and transpiration analyses: the roles of tree size and hydraulic lift. *Tree Physiology* 16:
 263-272. doi:10.1093/treephys/16.1-2.263.

Dawson, T.E., S. Mambelli, A.H. Plamboeck, P.H. Templer and K.P. Tu. 2002. Stable isotopes
 in plant ecology. *Annual Review of Ecology and Systematics* 33: 507-559.

de Groot, P.A. 2009. *Handbook of stable isotope analytical techniques* Elsevier, New York.

De Laeter, J.R., J.K. Böhlke, P. De Bièvre, H. Hidaka, H.S. Peiser, K.J.R. Rosman, et al. 2003.
 Atomic weights of the elements: Review 2000. *Pure and Applied Chemistry* 75: 683-800.

Ehleringer, J. and T.E. Dawson. 1992. Water uptake by plants: perspectives from stable isotope
 composition. *Plant Cell and Environment* 15: 1073-1082.

Ehleringer, J.R., S. Schwinning and R. Gebauer. 1999. Water use in arid land ecosystems. In: M.
 C. Press, editor *Advances in Plant Physiological Ecology*. Blackwell Science, Oxford. p.
 347-365.

Ellsworth, P.Z. and D.G. Williams. 2007. Hydrogen isotope fractionation during water uptake by
 woody xerophytes. *Plant and Soil* 291: 93-107. doi:10.1007/s11104-006-9177-1.

Feddes, R.A., H. Hoff, M. Bruen, T. Dawson, P. de Rosnay, P. Dirmeyer, et al. 2001. Modeling
 root water uptake in hydrological and climate models. *Bulletin of the American
 Meteorological Society* 82: 2797-2809.

Flanagan, L.B. and J.R. Ehleringer. 1991. Stable isotope composition of stem and leaf water:
 applications to the study of plant water use. *Functional Ecology* 5: 270-277.

Gat, J.R. 1996. Oxygen and hydrogen isotopes in the hydrologic cycle. *Annual Review of Earth
 and Planetary Sciences* 24: 225-262.

740 Gee, G.W., M.D. Campbell, G.S. Campbell and J.H. Campbell. 1992. Rapid measurement of low
 741 soil-water potential using a water activity meter. *Soil Science Society of America Journal*
 742 56: 1068-1070.

743 Gonfiantini, R. 1978. Standards for stable isotope measurements in natural compounds. *Nature*
 744 271: 534-536. doi:10.1038/271534a0.

745 Griffis, T., J. Baker, S. Sargent, B. Tanner and J. Zhang. 2004. Measuring field-scale isotopic
 746 CO₂ fluxes with tunable diode laser absorption spectroscopy and micrometeorological
 747 techniques. *Agricultural and Forest Meteorology* 124: 15-29.

748 Griffis, T.J., S.D. Sargent, X. Lee, J.M. Baker, J. Greene, M. Erickson, et al. 2010. Determining
 749 the oxygen isotope composition of evapotranspiration using eddy covariance. *Boundary-*
 750 *Layer Meteorology* 137: 307-326.

751 Han, L.-F., M. Groening, P. Aggarwal and B.R. Helliker. 2006. Reliable determination of
 752 oxygen and hydrogen isotope ratios in atmospheric water vapour adsorbed on 3A
 753 molecular sieve. *Rapid Communications in Mass Spectrometry* 20: 3612-3618.
 754 doi:10.1002/rcm.2772.

755 Hanisco, T.F., E.J. Moyer, E.M. Weinstock, J.M. St. Clair, D.S. Sayres, J.B. Smith, et al. 2007.
 756 Observations of deep convective influence on stratospheric water vapor and its isotopic
 757 composition. *Geophysical Research Letters* 34: L04814. doi:10.1029/2006gl027899.

758 Harmathy, T.Z. 1969. Simultaneous moisture and heat transfer in porous systems with particular
 759 reference to drying. National Research Council of Canada. Ottawa. Research Paper No.
 760 407.

761 Haverd, V. and M. Cuntz. 2010. Soil–Litter–Iso: A one-dimensional model for coupled transport
 762 of heat, water and stable isotopes in soil with a litter layer and root extraction. *Journal of*
 763 *Hydrology* 388: 438-455.

764 Haverd, V., M. Cuntz, D. Griffith, C. Keitel, C. Tados and J. Twining. 2011. Measured
 765 deuterium in water vapour concentration does not improve the constraint on the
 766 partitioning of evapotranspiration in a tall forest canopy, as estimated using a soil
 767 vegetation atmosphere transfer model. *Agricultural and Forest Meteorology* 151: 645-
 768 654. doi:10.1016/j.agrformet.2011.02.005.

769 Helliker, B.R. and S.L. Richter. 2008. Subtropical to boreal convergence of tree-leaf
 770 temperatures. *Nature* 454: 511-514.

771 Helliker, B.R., J.S. Roden, C. Cook and J.R. Ehleringer. 2002. A rapid and precise method for
 772 sampling and determining the oxygen isotope ratio of atmospheric water vapor. *Rapid*
 773 *Communications in Mass Spectrometry* 16: 929-932. doi:10.1002/rcm.659.

774 Henschel, J.R. and M.K. Seely. 2008. Ecophysiology of atmospheric moisture in the Namib
 775 Desert. *Atmospheric Research* 87: 362-368.

776 Herbstritt, B., B. Gralher and M. Weiler. 2012. Continuous in situ measurements of stable
 777 isotopes in liquid water. *Water Resources Research* 48: W03601.

778 Hesterberg, R. and U. Siegenthaler. 1991. Production and stable isotopic composition of CO₂ in
 779 a soil near Bern, Switzerland. *Tellus* 43B: 197-205.

780 Hoffmann, G., J. Jouzel and V. Masson. 2000. Stable water isotopes in atmospheric general
 781 circulation models. *Hydrological Processes* 14: 1385-1406.

782 Horita, J. 2005. Saline waters. In: P. K. Aggarwal, J. R. Gat and K. F. O. Froehlich, editors,
 783 Isotopes in the water cycle: Past, present and future of a developing science. IAEA,
 784 Netherlands. p. 271-287.

785 Horita, J., K. Rozanski and S. Cohen. 2008. Isotope effects in the evaporation of water: a status
 786 report of the Craig-Gordon model. *Isotopes in Environmental and Health Studies* 44: 23-
 787 49. doi:10.1080/10256010801887174.

788 Horita, J. and D.J. Wesolowski. 1994. Liquid-vapor fractionation of oxygen and hydrogen
 789 isotopes of water from the freezing to the critical temperature. *Geochimica et*
 790 *Cosmochimica Acta* 58: 3425-3437. doi:10.1016/0016-7037(94)90096-5.

791 Hsieh, J.C.C., S.M. Savin, E.F. Kelly and O.A. Chadwick. 1998. Measurement of soil-water $\delta^{18}\text{O}$
 792 values by direct equilibration with CO_2 . *Geoderma* 82: 255-268.

793 2010. Measurements of CO_2 carbon stable isotopes at artificial and natural analog sites. AGU
 794 Fall Meeting, San Francisco.

795 Jackson, R., L. Moore, W. Hoffman, W. Pockman and C. Linder. 1999. Ecosystem rooting depth
 796 determined with caves and DNA. *Proceedings of the National Academy of Sciences* 96:
 797 11387-11392.

798 Jacob, H. and C. Sonntag. 1991. An 8-year record of the seasonal variation of H-2 and O-18 in
 799 atmospheric water vapor and precipitation at Heidelberg, Germany. *Tellus Series B-*
 800 *Chemical and Physical Meteorology* 43: 291-300. doi:10.1034/j.1600-0889.1991.t01-2-
 801 00003.x.

802 Japas, M.L., R. Fernandez-Prini, J. Horita and D.J. Wesolowski. 1995. Fractioning of isotopic
 803 species between coexisting liquid and vapor water: Complete temperature range,

804 including the asymptotic critical behavior. *Journal of Physical Chemistry* 99: 5171-5175.
805 doi:10.1021/j100014a043.

806 Jouzel, J. and R.D. Koster. 1996. A reconsideration of the initial conditions used for stable water
807 isotope models. *Journal of Geophysical Research-Atmospheres* 101: 22933-22938.
808 doi:10.1029/96jd02362.

809 Keeling, C.D. 1958. The concentration and isotopic abundances of atmospheric carbon dioxide
810 in rural areas. *Geochimica et Cosmochimica Acta* 13: 322-324.

811 Kelly, S.F. and J.S. Selker. 2001. Osmotically driven water vapor transport in unsaturated soils.
812 *Soil Science Society of America Journal* 65: 1634-1641.

813 Kerstel, E.R.T., R. van Trigt, N. Dam, J. Reuss and H.A.J. Meijer. 1999. Simultaneous
814 determination of the H-2/H-1, O-17/O-16, and O-18/O-16 isotope abundance ratios in
815 water by means of laser spectrometry. *Analytical Chemistry* 71: 5297-5303.
816 doi:10.1021/ac990621e.

817 Kim, K. and X. Lee. 2011. Isotopic enrichment of liquid water during evaporation from water
818 surfaces. *Journal of Hydrology* 399: 364-375. doi:10.1016/j.jhydrol.2011.01.008.

819 Lee, J.-E., I. Fung, D.J. DePaolo and C.C. Henning. 2007. Analysis of the global distribution of
820 water isotopes using the NCAR atmospheric general circulation model. *Journal of*
821 *Geophysical Research* 112: D16306.

822 Lee, X. and W. Massman. 2011. A perspective on thirty years of the Webb, Pearman and
823 Leuning density corrections. *Boundary-Layer Meteorology* 139: 39-59.

824 Lee, X., S. Sargent, R. Smith and B. Tanner. 2005. In situ measurements of the water vapor
825 $^{18}\text{O}/^{16}\text{O}$ isotope ratio for atmospheric and ecological applications. *Journal of Atmospheric*
826 *and Oceanic Technology* 22: 555-565.

827 Luz, B., E. Barkan, R. Yam and A. Shemesh. 2009. Fractionation of oxygen and hydrogen
 828 isotopes in evaporating water. *Geochimica et Cosmochimica Acta* 73: 6697-6703.
 829 doi:10.1016/j.gca.2009.08.008.

830 Majoube, M. 1971. Oxygen-18 and deuterium fractionation between water and steam. *Journal De*
 831 *Chimie Physique Et De Physico-Chimie Biologique* 68: 1423-1438.

832 Mathieu, R. and T. Bariac. 1996. A numerical model for the simulation of stable isotope profiles
 833 in drying soils. *Journal of Geophysical Research* 101: 685-696.

834 Melayah, A., L. Bruckler and T. Bariac. 1996a. Modeling the transport of water stable isotopes
 835 in unsaturated soils under natural conditions .1. Theory. *Water Resources Research* 32:
 836 2047-2054. doi:10.1029/96wr00674.

837 Melayah, A., L. Bruckler and T. Bariac. 1996b. Modeling the transport of water stable isotopes
 838 in unsaturated soils under natural conditions .2. Comparison with field experiments.
 839 *Water Resources Research* 32: 2055-2065. doi:10.1029/96wr00673.

840 Merlivat, L. 1978. Molecular diffusivities of H_2^{16}O , HD^{16}O , and $\text{H}_2\text{O}-^{18}\text{O}$ in gases. *Journal of*
 841 *Chemical Physics* 69: 2864-2871. doi:10.1063/1.436884.

842 Midwood, A.J., B. Thornton and P. Millard. 2008. Measuring the (^{13}C) content of soil-respired
 843 CO_2 using a novel open chamber system. *Rapid Communications in Mass*
 844 *Spectrometry* 22: 2073-2081. doi:10.1002/rcm.3588.

845 Mooney, H.A., S.L. Gulmon, P.W. Rundel and J. Ehleringer. 1980. Further Observations on the
 846 Water Relations of *Prosopis-Tamarugo* of the Northern Atacama Desert. *Oecologia* 44:
 847 177-180.

848 Nicholson, S. 2000. Land surface processes and sahel climate. *Reviews of Geophysics* 38: 117-
 849 139.

850 Ogée, J., P. Peylin, M. Cuntz, T. Bariac, Y. Brunet, P. Berbigier, et al. 2004. Partitioning net
851 ecosystem carbon exchange into net assimilation and respiration with canopy-scale
852 isotopic measurements: An error propagation analysis with $^{13}\text{CO}_2$ and CO^{18}O data.
853 Global Biogeochemical Cycles 18: GB2019. doi:10.1029/2003gb002166.

854 Oi, T. 2003. Vapor pressure isotope effects of water studied by molecular orbital calculations.
855 Journal of Nuclear Science and Technology 40: 517-523. doi:10.3327/jnst.40.517.

856 Panday, S. and P.S. Huyakorn. 2008. MODFLOW SURFACT: A state-of-the-art use of vadose
857 zone flow and transport equations and numerical techniques for environmental
858 evaluations. Vadose Zone Journal 7: 610-631.

859 Peters, L.I. and D. Yakir. 2010. A rapid method for the sampling of atmospheric water vapour
860 for isotopic analysis. Rapid Communications in Mass Spectrometry 24: 103-108.
861 doi:10.1002/rcm.4359.

862 Philip, J.R. and D.A. de Vries. 1957. Moisture movement in porous materials under temperature
863 gradients. Transactions of the American Geophysical Union 38: 222–232.

864 Phillips, F.M. and H.W. Bentley. 1987. Isotopic fractionation during ion filtration: 1. Theory.
865 Geochimica et Cosmochimica Acta 51: 683-695.

866 Pollack, W., L.E. Heidt, R. Lueb and D.H. Ehhalt. 1980. Measurement of stratospheric water
867 vapour by cryogenic collection. Journal of Geophysical Research 85: 5555-5568.

868 Polyakov, V.B., J. Horita, D.R. Cole and A.A. Chialvo. 2007. Novel corresponding-states
869 principle approach for the equation of state of isotopologues: $(\text{H}_2\text{O})\text{-O-}^{18}$ as an example.
870 Journal of Physical Chemistry B 111: 393-401. doi:10.1021/jp064055k.

871 Richard, T., L. Mercury, M. Massault and J.L. Michelot. 2007. Experimental study of D/H
872 isotopic fractionation factor of water adsorbed on porous silica tubes. *Geochimica et*
873 *Cosmochimica Acta* 71: 1159-1169.

874 Risi, C., S. Bony, F. Vimeux, C. Frankenberg, D. Noone and J. Worden. 2010a. Understanding
875 the Sahelian water budget through the isotopic composition of water vapor and
876 precipitation. *Journal of Geophysical Research-Atmospheres* 115: D24110.
877 doi:10.1029/2010jd014690.

878 Risi, C., S. Bony, F. Vimeux and J. Jouzel. 2010b. Water-stable isotopes in the LMDZ4 general
879 circulation model: Model evaluation for present-day and past climates and applications to
880 climatic interpretations of tropical isotopic records. *Journal of Geophysical Research-*
881 *Atmospheres* 115: D24123. doi:10.1029/2010jd015242.

882 Rodriguez-Iturbe, I. and A. Porporato. 2004. *Ecohydrology of water-controlled ecosystems: Soil*
883 *moisture and plant dynamics* Cambridge University Press, Cambridge.

884 Rothfuss, Y., P. Biron, I. Braud, L. Canale, J.-L. Durand, J.-P. Gaudet, et al. 2010. Partitioning
885 evapotranspiration fluxes into soil evaporation and plant transpiration using water stable
886 isotopes under controlled conditions. *Hydrological Processes* 24: 3177-3194.
887 doi:10.1002/hyp.7743.

888 Rozanski, K. 2005. Isotopes in atmospheric moisture. In: P. K. Aggarwal, J. R. Gat and K. F. O.
889 Froehlich, editors, *Isotopes in the water cycle: Past, present and future of a developing*
890 *science*. IAEA, Netherlands. p. 291-302.

891 Scanlon, T.M., K.K. Caylor, S. Levin and I. Rodriguez-Iturbe. 2007. Positive feedbacks promote
892 power-law clustering of Kalahari vegetation. *Nature* 449: 209-213.

893 Schneider, M., K. Yoshimura, F. Hase and T. Blumenstock. 2010. The ground-based FTIR
 894 network's potential for investigating the atmospheric water cycle. *Atmospheric Chemistry*
 895 *and Physics* 10: 3427-3442.

896 Scrimgeour, C.M. 1995. Measurement of plant and soil water isotope composition by direct
 897 equilibration methods. *Journal of Hydrology* 173: 261-274.

898 Shurbaji, A.R.M. and F.M. Phillips. 1995. A numerical-model for the movement of H₂O, H₂¹⁸O,
 899 and ²HHO in the unsaturated zone. *Journal of Hydrology* 171: 125-142.

900 Sofer, Z. and J.R. Gat. 1975. Isotope composition of evaporating brines - effect of isotopic
 901 activity ratio in saline solutions. *Earth and Planetary Science Letters* 26: 179-186.

902 Stewart, G.L. 1972. Clay-water interaction, behavior of ³H and ²H in adsorbed water, and isotope
 903 effect. *Soil Science Society of America Proceedings* 36: 421-426.

904 Striegl, R.G. 1988. Distribution of gases in the unsaturated zone at a low-level radioactive-waste
 905 disposal site near Sheffield, Illinois. U.S. Geological Survey. Urbana, Illinois. Water-
 906 Resources Investigations Report 88-4025.

907 Syvertsen, J.P., G.L. Cunningham and T.V. Feather. 1975. Anomalous diurnal patterns of stem
 908 xylem water potentials in *Larrea tridentata*. *Ecology* 56: 1423-1428.

909 Tang, K.L. and X.H. Feng. 2001. The effect of soil hydrology on the oxygen and hydrogen
 910 isotopic compositions of plants' source water. *Earth and Planetary Science Letters* 185:
 911 355-367.

912 Twining, J., D. Stone, C. Tadros, A. Henderson-Sellers and A. Williams. 2006. Moisture
 913 Isotopes in the Biosphere and Atmosphere (MIBA) in Australia: A priori estimates and
 914 preliminary observations of stable water isotopes in soil, plant and vapour for the
 915 Tumbarumba Field Campaign. *Global and Planetary Change* 51: 59-72.

916 Walker, G.R., P.H. Woods and G.B. Allison. 1994. Interlaboratory comparison of methods to
 917 determine the stable isotope composition of soil water. *Chemical Geology* 111: 297-306.

918 Wang, L., K. Caylor and D. Dragoni. 2009. On the calibration of continuous, high-precision $\delta^{18}\text{O}$
 919 and $\delta^2\text{H}$ measurements using an off-axis integrated cavity output spectrometer. *Rapid*
 920 *Communications in Mass Spectrometry* 23: 530-536.

921 Wang, L., K.K. Caylor, J. Camilo Villegas, G.A. Barron-Gafford, D.D. Breshears and T.E.
 922 Huxman. 2010. Partitioning evapotranspiration across gradients of woody plant cover:
 923 assessment of a stable isotope technique. *Geophysical Research Letters* 37: L09401.
 924 doi:10.1029/2010GL043228.

925 Wang, L., S. Good, K. Caylor and L.A. Cernusak. 2012. Direct quantification of leaf
 926 transpiration isotopic composition. *Agricultural and Forest Meteorology* 154-155: 127-
 927 135.

928 Warren, J., J. Brooks, M. Dragila and F. Meinzer. 2011. In situ separation of root hydraulic
 929 redistribution of soil water from liquid and vapor transport. *Oecologia* 166: 899-911.

930 Wassenaar, L.I., M.J. Hendry, V.L. Chostner and G.P. Lis. 2008. High resolution pore water $\delta^2\text{H}$
 931 and $\delta^{18}\text{O}$ measurements by $\text{H}_2\text{O}_{(\text{liquid})}$ - $\text{H}_2\text{O}_{(\text{vapor})}$ equilibration laser spectroscopy.
 932 *Environmental Science & Technology* 42: 9262-9267. doi:10.1021/es802065s.

933 Webster, C.R. and A.J. Heymsfield. 2003. Water isotope ratios D/H, $^{18}\text{O}/^{16}\text{O}$, $^{17}\text{O}/^{16}\text{O}$ in and out
 934 of clouds map dehydration pathways. *Science* 302: 1742-1745.

935 Welp, L.R., R.F. Keeling, H.A.J. Meijer, A.F. Bollenbacher, S.C. Piper, K. Yoshimura, et al.
 936 2011. Interannual variability in the oxygen isotopes of atmospheric CO_2 driven by El
 937 Nino. *Nature* 477: 579-582.

938 West, A.G., S.J. Partrickson and J.R. Ehleringer. 2006. Water extraction times for plant and soil
 939 materials used in stable isotope analysis. *Rapid Communications in Mass Spectrometry*
 940 20: 1317-1321.

941 White, J.W.C., E.R. Cook, J.R. Lawrence and W.S. Broecker. 1985. The D/H ratios of sap in
 942 trees: Implications for water sources and tree ring D/H ratios. *Geochimica Et*
 943 *Cosmochimica Acta* 49: 237-246.

944 Wingate, L., J. Ogée, M. Cuntz, B. Genty, I. Reiter, U. Seibt, et al. 2009. The impact of soil
 945 microorganisms on the global budget of $d^{18}O$ in atmospheric CO_2 . *Proceedings of the*
 946 *National Academy of Sciences* 106: 22411-22415.

947 Wingate, L., U. Seibt, K. Maseyk, J. Ogée, P. Almeida, D. Yakir, et al. 2008. Evaporation and
 948 carbonic anhydrase activity recorded in oxygen isotope signatures of net CO_2 fluxes from
 949 a Mediterranean soil. *Global Change Biology* 14: 2178-2193.

950 Worden, J., D. Noone, K. Bowman and T.E. Spect. 2007. Importance of rain evaporation and
 951 continental convection in the tropical water cycle. *Nature* 445: 528-532. doi:Doi
 952 10.1038/Nature05508.

953 Yakir, D. and L.D.L. Sternberg. 2000. The use of stable isotopes to study ecosystem gas
 954 exchange. *Oecologia* 123: 297-311.

955 Yakir, D. and X.-F. Wang. 1996. Fluxes of CO_2 and water between terrestrial vegetation and the
 956 atmosphere estimated from isotope measurements. *Nature* 380: 515-517.

957 Yamanaka, T. and R. Shimizu. 2007. Spatial distribution of deuterium in atmospheric water
 958 vapor: Diagnosing sources and the mixing of atmospheric moisture. *Geochimica et*
 959 *Cosmochimica Acta* 71: 3162-3169.

960 Yepez, E., D. Williams, R. Scott and G. Lin. 2003. Partitioning overstory and understory
 961 evapotranspiration in a semiarid savanna woodland from the isotopic composition of
 962 water vapor. *Agricultural and Forest Meteorology* 119: 53-68.
 963 Yoshimura, K., S. Miyazaki, S. Kanae and T. Oki. 2006. Iso-MATSIRO, a land surface model
 964 that incorporates stable water isotopes. *Global and Planetary Change* 51: 90-107.
 965 doi:10.1016/j.gloplacha.2005.12.007.
 966 Yu, W., T. Yao, L. Tian, Y. Wang and C. Yin. 2005. Isotopic composition of atmospheric water
 967 vapor before and after the monsoon's end in the Nagqu River Basin. *Chinese Science*
 968 *Bulletin* 50: 2755-2760.
 969 Zimmerman, U., D. Ehhalt and K.O. Munnich. 1967. Soil-water movement and
 970 evapotranspiration: Changes in the isotopic composition of the water. In: IAEA, editor
 971 *Isotopes in hydrology; Proceedings of the symposium (1966: Vienna)*. International
 972 Atomic Energy Agency, Vienna. p. 567-585.
 973
 974

975 Table 1: Summary of measurement and modeling techniques to quantify isotopic compositions
 976 of soil water vapor and soil evaporation.

Potential methods	Notes	References
Measurement:		
Isothermal equilibrium (H ₂ O, CO ₂ , H ₂)†	Inside the laboratory	Stewart 1972, Scrimgeour 1995, Hsieh et al. 1998, Richard et al. 2007, Wassenaar et al. 2008
<i>In situ</i> CO ₂ -H ₂ O equilibrium†	In vadose zone	Hesterberg and Siegenthaler 1991, Hsieh et al. 1998, Tang and Feng 2001, Wingate et al. 2008
Cryogenic soil column vapor collection	Inside the laboratory	Zimmerman 1967, Stewart 1972, Braud et al. 2009ab; Rothfuss et al. 2010
<i>In situ</i> cryogenic soil gas sampling	In vadose zone	Striegl 1988, references in Mathieu and Bariac 1996
<i>In situ</i> sealed chamber	From soil surface	Haverd et al. 2011
Open chamber with mass balance	From soil surface	Wang et al. 2012
<i>In situ</i> direct measurement with laser spectroscopy	In vadose zone	This manuscript
Modeling:		
Craig-Gordon Model	Formulated for free water evaporation	Craig and Gordon 1965, Horita et al. 2008
Analytical isotope transport models		Zimmerman et al. 1967, Barnes and Allison 1983
Numerical isotope transport models	Varied results, but capture the shape of observations well	Shurbaji and Phillips 1995, Mathieu and Bariac 1996, Melayah et al. 1996a,b, Braud et al. 2005a,b, Braud et al. 2009ab, Harverd and Cuntz 2010, Haverd et al. 2011

977 † - These methods are used to estimate liquid soil water isotopic composition, but the details of
 978 the equilibrium and sampling methods are relevant to soil water vapor isotopes.

Table 2: Liquid-vapor isotopic fractionation factors for water. See Horita et al. (2008) for compiled historical values. Equilibrium values are listed for 25 °C unless noted.

	$\alpha_{LV}(^{18}\text{O})$	$\alpha_{LV}(^2\text{H})$	Description	Ref.
Equilibrium:				
Best current values (empirical)	1.00935	1.07875	Combination of evaporation experiments	1
<i>ab initio</i>	<i>1.008†</i>	<i>1.107</i>	<i>HF calculation level</i>	2
<i>ab initio</i>	<i>1.013</i>	<i>1.145</i>	<i>B3LYP calculation level</i>	2
<i>Molecular simulation</i>	<i>1.016</i>	<i>1.622</i>	<i>Gaussian charge polarizable</i>	3
<i>Molecular simulation</i>	<i>1.018</i>	<i>1.612</i>	<i>Nonpolarizable extended simple point charge</i>	3
<i>Thermodynamics</i>	<i>1.0094</i>	<i>1.0798</i>	<i>Corresponding states principle</i>	4,5
Empirical - dried clay	NA	1.04‡	See text	6
Empirical - silica tubes	NA	1.055§	See text	7
Kinetic (<i>D/Di</i>):				
Best current values (empirical)	1.0285	1.0251	Evaporation at 20 °C in air	8
	1.0281	1.0249	Evaporation at 20 °C in N2	8
Recent experiment	1.0275	1.0230	Values from the 20.1 °C experiment in air	9
<i>Gas kinetic theory</i>	<i>1.0323</i>	<i>1.0166</i>	<i>In dry air; Isotopologues have identical collision diameters</i>	10
<i>Gas kinetic theory</i>	<i>1.0319</i>	<i>1.0164</i>	<i>In N2; Isotopologues have identical collision diameters</i>	11

Italics indicate modeled values.

References: 1 - Horita and Wesolowski 1994; 2 - Oi 2003; 3 - Chialvo and Horita 2009; 4 - Japas et al. 1995; 5 - Polyakov et al. 2007; 6 - Stewart 1972; 7 - Richard et al. 2007; 8 - Merlivat 1978; 9 - Luz et al. 2009; 10 - Horita et al. 2008; 11 - Cappa et al. 2003

† – All equilibrium model values (*ab initio*, molecular dynamic, and thermodynamic) are estimated from Figures 4, 6 and 8 from Chialvo and Horita (2009); *ab initio* means “from first principles”

‡ - Temperature unknown -- listed as "room temperature"; the listed $\alpha_{LV}(^2\text{H})$ value (1.04) is the median of 0.93 to 1.06 ($n = 7$), see text for details.

991 § - Temperature is 20 °C rather than 25 °C. The free water $\alpha_{L/V}(^2H)$ value at 20 °C is 1.08453
992 from Equation 3. The listed value (1.055) was the maximum observed, corresponding to relative
993 humidity (RH) values above ~70%. Lower RH conditions corresponded to lower values of
994 $\alpha_{L/V}(^2H)$ down to around 1.30 at 10% RH.

995

996 Table 3: Craig-Gordon model parameters, and example calculations of δ_E for free water and soil
 997 water. The example data were collected on 29 March 2011 at Mpala Research Center, Kenya,
 998 from a soil profile fitted with buried Teflon tubing from which air was drawn directly into a
 999 Water Vapor Isotope Analyzer (DLT-100, Los Gatos Research Inc., Mountain View, CA).

Parameter	Example – Mean of 5, 10, 20, and 30 cm		Example – 5 cm		Typical range	
T_A	302		302		280 to 310	
T_0	300		301		290 to 320	
h_A	0.331		0.331		0.2 to 0.6	
$h_A'(T)$	0.374		0.351		0.2 to 1.0	
$h_A'(T, \psi)$	0.429		0.433			
ψ_0	-18.8		-29.2		-1 to -100	
θ_0	0.0602		0.0525		0.01 to 0.45	
θ_s	0.45		0.45		0.2 to 0.5	
θ_r	0.035		0.035		0.01 to 0.05	
Depth min [cm]	5		5		10 to 50‡	
Depth max [cm]	30		5			
$n(\theta)$	0.970		0.979		0.5 to 1.0	
n (free water)	0.5		0.5		0.5	
	$\delta^{18}\text{O}$	$\delta^2\text{H}$	$\delta^{18}\text{O}$	$\delta^2\text{H}$	$\delta^{18}\text{O}$	$\delta^2\text{H}$
$\alpha_{e,L/V}$	1.009206	1.07693	1.009117	1.07579	1.008 to 1.010	1.059 to 1.088
D/D_i	1.0285	1.0251	1.0285	1.0251	1.028 to 1.032	1.016 to 1.025
$\varepsilon_{k,L/V}(\theta, T)$	0.01728	0.01523	0.01810	0.01596	0.001 to 0.023	0.001 to 0.020
$\varepsilon_{k,L/V}(\theta, T, \psi)$	0.01578	0.01391	0.01581	0.01394		
$\varepsilon_{k,L/V}(\text{free water}, T)$	0.00891	0.00786	0.00925	0.00815	0.001 to 0.014	0.001 to 0.013
r_m/r	1	1	1	1	0.5 to 1.0	0.5 to 1.0
δ_L	6.2†	6.5	13.2	26.2	-5 to 10	-30 to 30
δ_V (meas)	-2.8	-56.6	-2.2	-54.6	NA	NA
δ_V (equil)	-3.0	-65.4	4.1	-46.1	-15 to 3.0	-120 to -30
δ_A	-10.4	-68.7	-10.4	-68.7	-10 to -20	-50 to -150
Calculated Evaporate:						
$\delta_E(\theta, T)$	-25.6	-94.3	-15.7	-65.1		
$\delta_E(\theta, T, \psi)$	-24.5	-94.6	-12.6	-61.3		
$\delta_E(\text{free water}, T)$	-12.7	-83.7	-2.5	-54.0		

1000 ‡ Typical evaporating front depth from Barnes and Allison (1988)

1001 † - All isotope values are presented here in per mil notation ($\delta \times 1000$), whereas in calculations
 1002 they are converted to decimal notation (e.g. Equation 4, resulting in -25.6 ‰ for “ $\delta_E(\theta, T)$ ” in
 1003 column 2 above):

$$1004 \quad \delta_E = \frac{(0.0062 / 1.009206) - 0.374(-0.0104) - 0.009206 - 0.01728}{1 - 0.374 + 0.01728} = -0.0256$$

1005

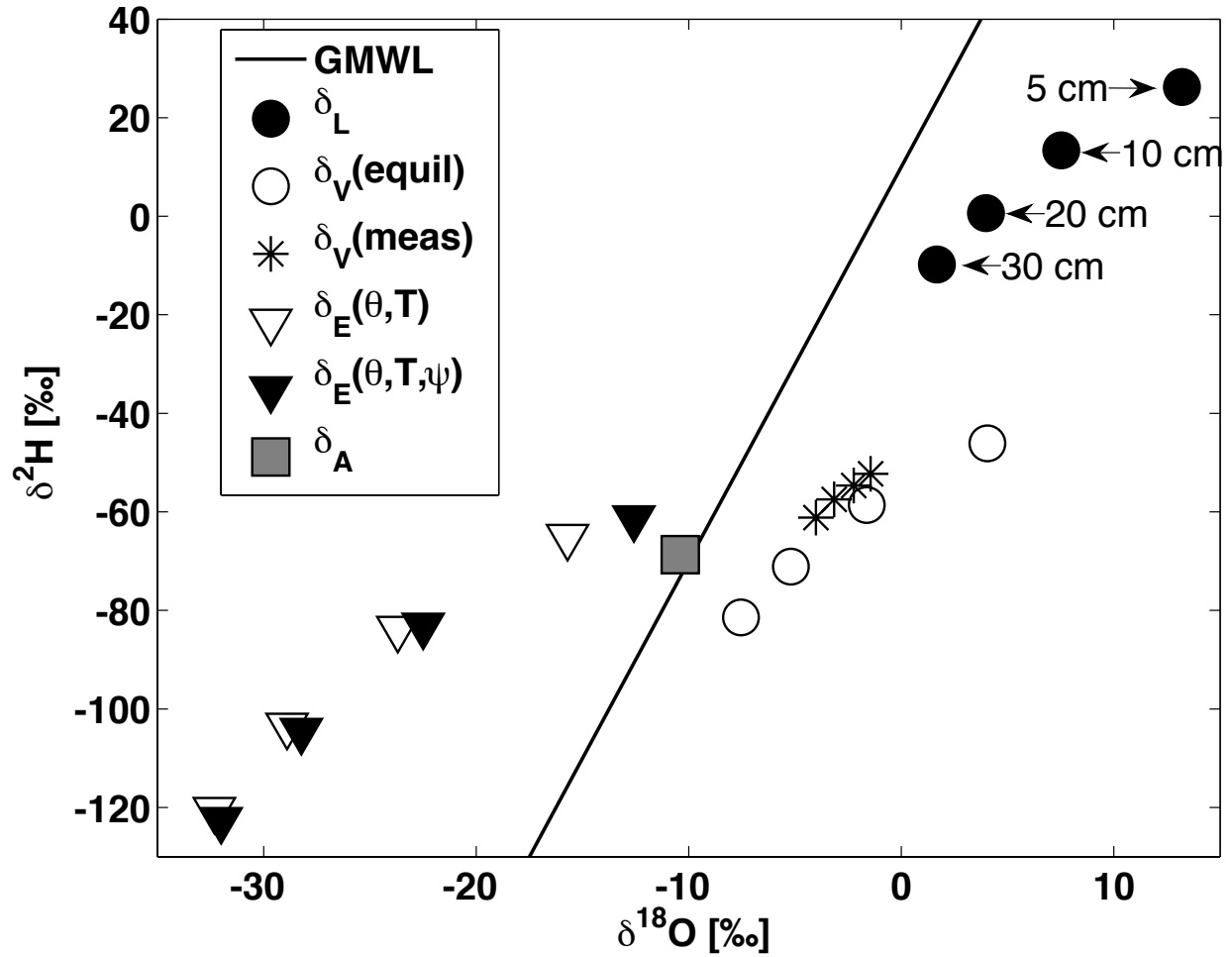


Figure 1: Measured and calculated isotope values of liquid and vapor phase water from a soil profile sampled 29 March 2011 in sandy loam soil at Mpala Research Center, Kenya (see Section 4 and Table 3). Sampling depths are shown for the liquid soil water samples, and each set of vapor values follows the same depth sequence. Two sets of δ_V values are shown: “ $\delta_V(\text{meas})$ ” was measured directly in the field with a Water Vapor Isotope Analyzer (DLT-100, Los Gatos Research Inc., Mountain View, CA); “ $\delta_V(\text{equil})$ ” was calculated using soil temperature and liquid soil water isotopic composition (Equations 1 to 3). Craig-Gordon model δ_E values were calculated in two ways: “ $\delta_E(\theta, T)$ ” was calculated conventionally, considering volumetric water

1015 content and soil temperature (Equations 2 to 8); “ $\delta_E(\theta, T, \psi)$ ” was calculated by additionally
1016 considering soil water potential (Equations 2 to 9).

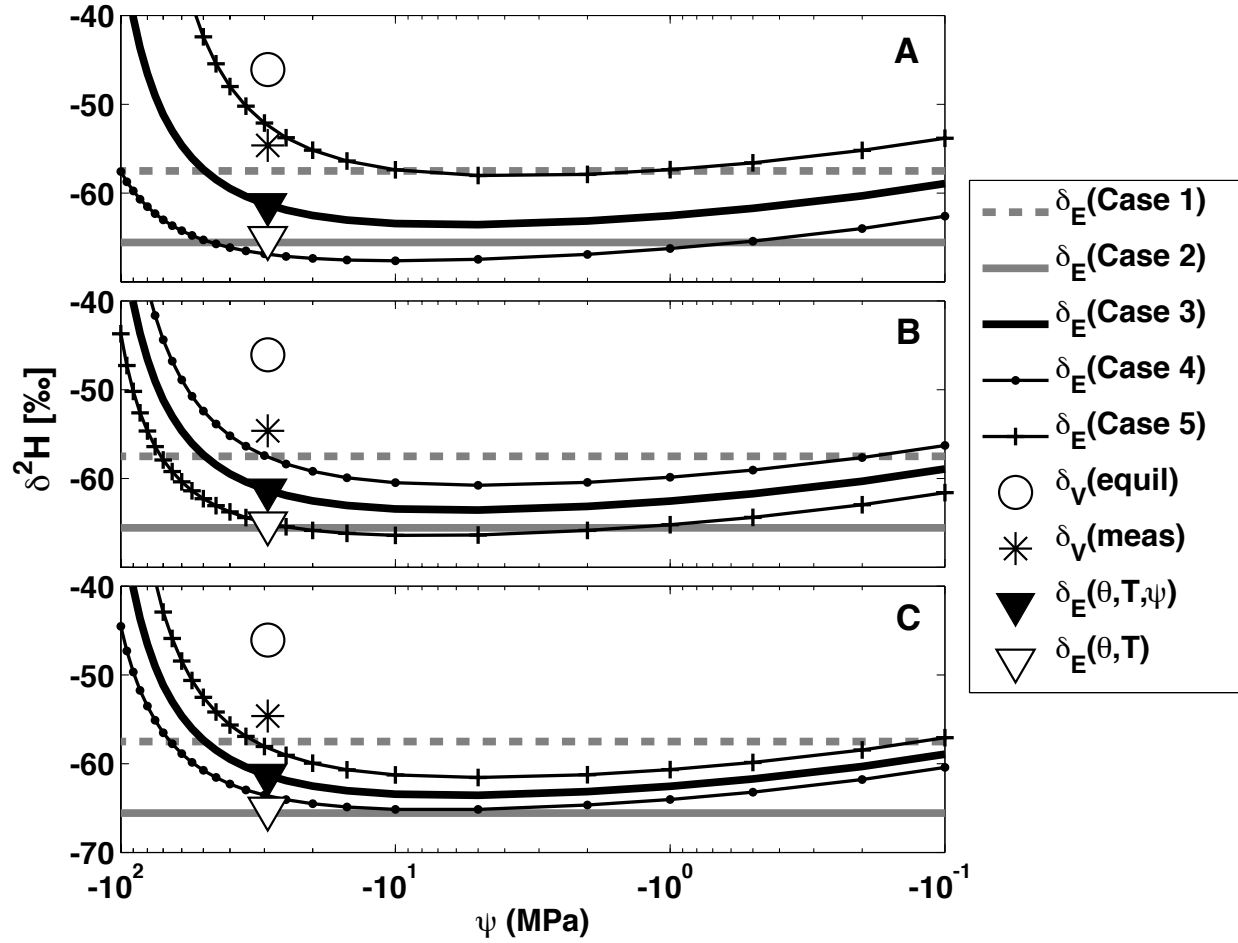


Figure 2: Craig-Gordon model calculations (Equations 2 to 9) for $\delta^2\text{H}$ across a range of soil water potentials (ψ) and ambient atmospheric parameters. The measured and calculated parameters for the 5 cm depth example of Table 3 and Figure 1 are used as a starting point, and these values are shown with the same symbols as in Figure 1. Each panel shows five “Cases.” Cases 1 and 2 were calculated without considering soil moisture content or soil water potential (i.e., $n = 1$ and $a_w = 1$), and use the contrasting α_k values of Cappa et al. (2003) and Merlivat (1978), respectively. Cases 3, 4 and 5 show the effects of varying one of three atmospheric parameters: relative humidity (h_A) in panel A, water vapor isotopic composition (δ_A) in panel B, and temperature (T_A) in panel C. Case 3 always uses the measured values ($h_A = 0.331$, $\delta_A = -68.7$

1027 ‰, $T_A = 28.8\text{ }^{\circ}\text{C}$), whereas Cases 4 and 5 use lower and higher bounds, respectively, of a range
1028 that one could expect in the field ($h_A \pm 0.1$, $\delta_A \pm 5\text{ ‰}$, and $T_A \pm 2\text{ }^{\circ}\text{C}$).

1029

1030